

Magnetic Transitions of Single-Component Molecular Metal [Au(tmdt)₂] and Its Alloy Systems

Biao Zhou,[†] Mina Shimamura,[†] Emiko Fujiwara,[†] Akiko Kobayashi,^{*,†} Takeshi Higashi,[§] Eiji Nishibori,[§] Makoto Sakata,[§] HengBo Cui,[‡] Kazuyuki Takahashi,[‡] and Hayao Kobayashi[†]

Research Centre for Spectrochemistry, Graduate School of Science, The University of Tokyo, Hongo, Bunkyo-ku, Tokyo 113-0033, Japan, Department of Applied Physics, Nagoya University, Nagoya 464-8603, Japan, and Institute for Molecular Science and JST-CREST, Myodaiji, Okazaki 444-8585, Japan

Received November 29, 2005; E-mail: akiko@chem.s.u-tokyo.ac.jp

[Ni(tmdt)₂] (tmdt = trimethylenetetrafulvalenedithiolate) is the first single-component molecular metal where metal electrons are automatically generated by self-assembly of neutral [Ni(tmdt)₂] molecules.¹ Recently, a rigorous experimental evidence for the existence of three-dimensional electron and hole Fermi surfaces was obtained by detecting the de Haas–van Alphen (dHvA) effect.² [Au(tmdt)₂] is isostructural to [Ni(tmdt)₂], but the electronic band structures of these two systems are completely different to each other because the neutral bis(dithiolato)gold complex has an odd number of total electrons. In fact, [Au(tmdt)₂] was reported to undergo a possible antiferromagnetic transition around 100 K without loss of its high conductivity.³ In this paper, we present detailed information on the antiferromagnetic transition of [Au(tmdt)₂] around 110 K (*T_N*) and its spin–flop behavior and the electromagnetic properties of the “molecular alloys” of [Ni(tmdt)₂] and [Au(tmdt)₂].

It is very difficult to prepare single crystals of [Au(tmdt)₂] with sufficient quality, but we have recently succeeded in obtaining the crystals with the size of about 30 μm. By the single-crystal X-ray structure determination using Rigaku VariMax Saturn70 X-ray system equipped with confocal mirror, we could determine the crystal structure. Unlike the Ni atom of [Ni(tmdt)₂], the Au atom was found to have a large temperature factor, indicating the possibility of large thermal motion perpendicular to the molecular plane and/or small deviation from the central position at room temperature. The susceptibility of newly obtained high-quality crystalline powder sample was re-examined by a SQUID magnetometer up to 50 kOe and down to 2 K. As shown in Figure 1, the susceptibility (χ) was 4.2×10^{-4} emu mol⁻¹ at room temperature, which is attributable to the paramagnetism of π metal electrons. Between 150 and 110 K, it decreased gradually from 4.0×10^{-4} to 3.6×10^{-4} emu mol⁻¹. And below 110 K, χ showed characteristic temperature and magnetic field dependences, suggesting an antiferromagnetic transition at 110 K (*T_N*), which is 10 K higher than the previously reported transition temperature. The *H* dependence of *M* was measured at 40 K because the accurate *M* values were hardly obtainable at low temperature because of paramagnetic impurities. As shown in the inset of Figure 1, the *H* dependences of *M* and *dM/dH* suggested the spin–flop transition around 23 kOe.

The *ab initio* electronic band calculation of [Au(tmdt)₂] suggested that the partial nesting of the Fermi surfaces occurs at *T_N*, and Fermi surface pockets remain in the magnetic phase.⁴ Consequently, it will be natural to assume that χ can be explained by the contributions from the antiferromagnetically ordered magnetic

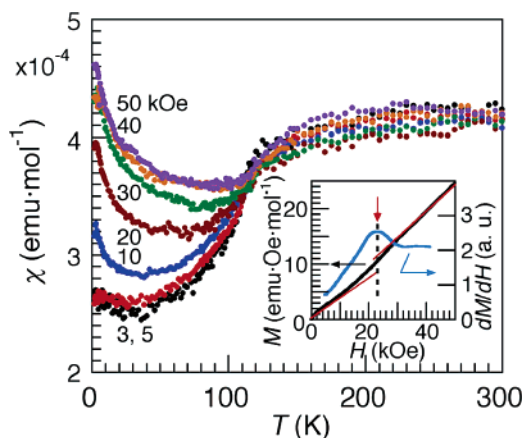


Figure 1. Temperature and magnetic field dependences of the susceptibilities of the crystalline powder sample of [Au(tmdt)₂]. The inset is the *H* dependences of *M* (black line) and *dM/dH* (blue line) at 40 K. The red arrow indicates the spin–flop field.

moments (χ_{AF}) and temperature-independent paramagnetism of conduction electrons (χ_p) ($\chi = \chi_{AF} + \chi_p$) at $T < T_N$ ($=110$ K). Then, the magnitude of the magnetic moment produced at *T_N* (μ_0) was roughly estimated from the magnitude of the decrease of the susceptibility below *T_N* by approximately assuming the well-known very simple relation of the powder sample of the antiferromagnet with the localized moment μ_0 [$\chi_{AF}(0 \text{ K})/\chi_{AF}(T_N) \approx 2/3$ at weak magnetic field, $\chi_{AF}(T_N) \approx \mu_0^2/(3k_B T_N)$]. As seen from Figure 1, χ decreased from about 3.6×10^{-4} to about 2.6×10^{-4} emu mol⁻¹ below *T_N* at low magnetic field. Thus, μ_0 was estimated to be about $0.30 \mu_B$. The large low-temperature magnetic susceptibility of 2.6×10^{-4} emu mol⁻¹ at low magnetic field is consistent with the theoretical calculation suggesting the existence of the Fermi surface pockets below *T_N*. To our best knowledge, [Au(tmdt)₂] is the first molecular conductor where the same π electrons bear electrical conductivity and magnetic order.

Since [Ni(tmdt)₂] and [Au(tmdt)₂] are isostructural to each other, we have tried to obtain the alloy systems [Ni_{1-x}Au_x(tmdt)₂]. Black microcrystals of [Ni_{1-x}Au_x(tmdt)₂] ($0.0 < x < 1.0$) were prepared by the electrochemical oxidation from the mixed solution of (Me₄N)₂[Ni(tmdt)₂] and (t⁺Bu₄N)[Au(tmdt)₂]. The synchrotron radiation powder X-ray diffraction experiments were performed because the size of the crystals of [Ni_{1-x}Au_x(tmdt)₂] was very small. The diffraction peaks were shifted systematically to the lower angle with the increase of Au concentration (*x*), and no extra peaks attributable to other phases were observed, showing that the alloys [Ni_{1-x}Au_x(tmdt)₂] with arbitrary mixing ratio could be synthesized. In the case of $x \approx 0.25$, the black plate-like tiny single crystals were obtained, and the single-crystal resistivity measurement of [Ni_{0.75}-

[†] The University of Tokyo.

[§] Nagoya University.

[‡] Institute for Molecular Science and JST-CREST.

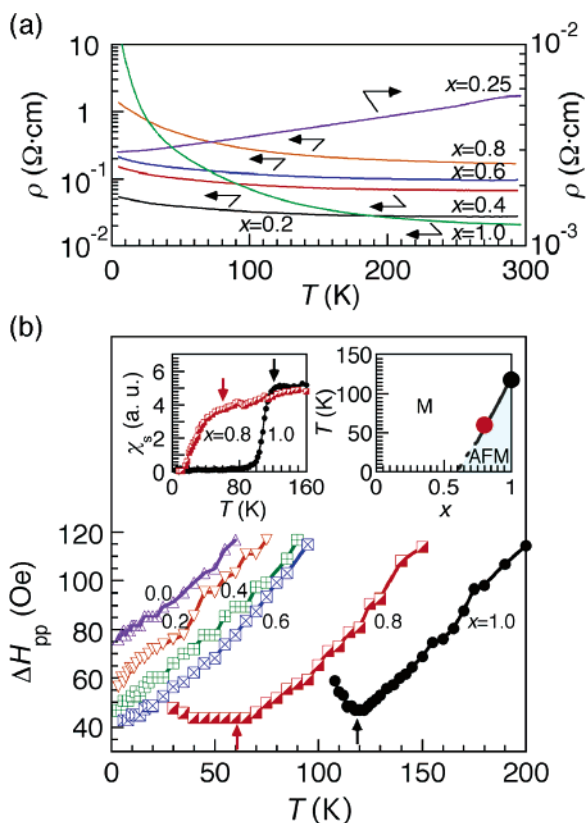


Figure 2. (a) The temperature dependences of the resistivities of compacted powder samples of $[\text{Ni}_{1-x}\text{Au}_x(\text{tmdt})_2]$ ($x = 0, 0.2, 0.4, 0.6, 0.8, 1.0$) and the single crystal of $[\text{Ni}_{0.75}\text{Au}_{0.25}(\text{tmdt})_2]$ ($x = 0.25$). (b) The temperature dependence of the peak-to-peak line width (ΔH_{pp}) of ESR of $[\text{Ni}_{1-x}\text{Au}_x(\text{tmdt})_2]$. The arrows indicate the on-set temperatures of antiferromagnetic phase transitions. The insets are the ESR intensities (left) and the T - x phase diagram (right) of $[\text{Ni}_{1-x}\text{Au}_x(\text{tmdt})_2]$: M = normal metal, AFM = antiferromagnetic metal.

$\text{Au}_{0.25}(\text{tmdt})_2$ was made down to 0.5 K by the four-probe method. The size of crystals was about $0.1 \times 0.05 \times 0.025 \text{ mm}^3$. The room-temperature conductivity was 180 S cm^{-1} . The resistivity decreased monotonically with lowering temperature, showing $[\text{Ni}_{0.75}\text{Au}_{0.25}(\text{tmdt})_2]$ to be really the “alloy” of single-component molecular conductors (Figure 2a). Similar to $[\text{Ni}(\text{tmdt})_2]$, the temperature dependence of the resistivity was very small: $\rho(4 \text{ K})/\rho(300 \text{ K}) \approx 3$ ($[\text{Ni}(\text{tmdt})_2]$ ¹ and 2 ($[\text{Ni}_{0.75}\text{Au}_{0.25}(\text{tmdt})_2]$).

The resistivities of compressed pellet samples of $[\text{Ni}_{1-x}\text{Au}_x(\text{tmdt})_2]$ were also measured down to 4 K (Figure 2a). The room-temperature conductivity of $[\text{Au}(\text{tmdt})_2]$ ($x = 1.0$) was 50 S cm^{-1} , which is more than three times larger than the previously reported value (15 S cm^{-1}).³ The room-temperature conductivities of the alloys with $x = 0.2$ – 0.8 were 40 – 10 S cm^{-1} , which tended to be smaller with increasing x . Compared with the conductivity of $[\text{Au}(\text{tmdt})_2]$, whose crystal quality was much improved by the many trials of

the sample purification, the conductivity of the alloys was relatively small, probably due to the relatively low sample quality and the possible effect of randomness of the distribution of $[\text{Ni}(\text{tmdt})_2]$ and $[\text{Au}(\text{tmdt})_2]$. The resistivities of $[\text{Ni}_{1-x}\text{Au}_x(\text{tmdt})_2]$ were almost temperature-independent down to 4 K for $x < 0.6$, despite of the compressed pellet samples. The sample with $x \approx 0.8$ showed a slight increase of the resistivity with lowering temperature, but the apparent activation energy was about 1 meV, indicating $[\text{Ni}_{1-x}\text{Au}_x(\text{tmdt})_2]$ to be essentially metallic at 4–300 K.

ESR spectra of polycrystalline samples of $[\text{Ni}_{1-x}\text{Au}_x(\text{tmdt})_2]$ were measured in the temperature range of 3.3–300 K. As shown in the inset of Figure 2b, ESR intensity of $[\text{Au}(\text{tmdt})_2]$ showed a sharp drop at 110 K (T_N), which agrees well with that of the susceptibility change obtained by the SQUID magnetometer (see Figure 1). The peak-to-peak line width (ΔH_{pp}) decreased with lowering temperature down to 120 K, below which ΔH_{pp} tended to increase (Figure 2b). Similar but much more sluggish behavior was also observed for $x \approx 0.8$, probably due to the random distribution of $[\text{Au}(\text{tmdt})_2]$ and $[\text{Ni}(\text{tmdt})_2]$ and the insufficient quality of sample. A slight increase of ΔH_{pp} around 60 K coincides with the onset of the gradual decrease of the ESR intensity, suggesting that T_N of $[\text{Ni}_{1-x}\text{Au}_x(\text{tmdt})_2]$ is lowered with decreasing x . The temperature dependence of ΔH_{pp} of the sample with $x \approx 0.6$ became very weak below 15 K, but no clear increase of ΔH_{pp} was observed.

In conclusion, the temperature dependence of the resistivities of the compressed pellet samples of the novel alloys of single-component molecular metals, $[\text{Ni}_{1-x}\text{Au}_x(\text{tmdt})_2]$, showed the system to be essentially metallic down to low temperature. In $[\text{Au}(\text{tmdt})_2]$, the antiferromagnetic transition was observed around 110 K (T_N), and in the Au-rich alloy ($x \approx 0.8$), the broad antiferromagnetic transition was observed around 60 K.

Acknowledgment. We thank Prof. Kanoda and Dr. Miyagawa for the information on their low-temperature ^1H NMR experiments, and Dr. K. Kato for the synchrotron radiation experiments at SPring-8 BL02B2 with approval of JASRI. This study was partially supported by a Grant-in-aid for Scientific Research (S) (14103005), Priority Areas of Molecular Conductors (No. 15073209) and by the 21st Century COE Program for Frontiers in Fundamental Chemistry from the Ministry of Education, Culture, Sports, Science and Technology.

References

- (1) (a) Tanaka, H.; Okano, Y.; Kobayashi, H.; Suzuki, W.; Kobayashi, A. *Science* **2001**, *291*, 285–287. (b) Kobayashi, A.; Tanaka, H.; Kobayashi, H. *J. Mater. Chem.* **2001**, *11*, 2078–2088. (c) Kobayashi, A.; Fujiwara, E.; Kobayashi, H. *Chem. Rev.* **2004**, *104*, 5243–5264.
- (2) Tanaka, H.; Tokumoto, M.; Ishibashi, S.; Okano, Y.; Graf, D.; Choi, E. S.; Brooks, J. S.; Yasuzuka, S.; Kobayashi, H.; Kobayashi, A. *J. Am. Chem. Soc.* **2004**, *126*, 10518–10519.
- (3) Suzuki, W.; Fujiwara, E.; Kobayashi, A.; Fujishiro, Y.; Nishibori, E.; Takata, M.; Sakata, M.; Fujiwara, H.; Kobayashi, H. *J. Am. Chem. Soc.* **2003**, *125*, 1486–1487.
- (4) Ishibashi, S.; Tanaka, H.; Kohyama, M.; Tokumoto, M.; Kobayashi, A.; Kobayashi, H.; Terakura, K. *J. Phys. Soc. Jpn.* **2005**, *74*, 843–846.

JA0581144